J Mater Sci (2009) 44:5824–5828
DOI 10.1007/s10853-009-3820-1

Preparation and properties of $Bi_6Ti_5WO_{22}$: a new phase in the Bi_2O_3–TiO_2–WO_3 system

T. Jardiel · A. C. Caballero · L. Fuentes · M. Villegas

Received: 12 March 2009 / Accepted: 18 August 2009 / Published online: 1 September 2009

Abstract In a recent report, the evaluation of the phase relations in the Bi_2O_3–TiO_2–WO_3 ternary system has shown the existence of a new phase with nominal composition close to $Bi_6Ti_5WO_{22}$. In the present contribution we attempt to prepare this single phase by using a solid state route. Although XRD analyses also show traces of two minority Aurivillius-type phases in the synthesized materials, the crystal structure of the $Bi_6Ti_5WO_{22}$ phase has been determined by Rietveld analyses revealing a complex structure similar to that of $Bi_3(AlSb_2)O_{11}$ and $PbHoAl_3O_8$ related compounds. The electrical response of this new phase was characterized as well. Three peaks are observed in its dielectric response: two of them positioned around 0 °C and can be assigned to this $Bi_6Ti_5WO_{22}$ structure. The third one rises up to 665 °C and confirms the presence of the Aurivillius-type phases.

Introduction

The distribution of phases in the Bi_2O_3–TiO_2–WO_3 system has been fairly studied because they exhibit a great diversity of applications. A great number of compounds belonging to the Aurivillius family have been found in this ternary system, including numerous ferroelectric materials with useful properties for optical memories, high temperature piezoelectric and electro-optic devices [1–4]. Aurivillius-type phases with nominal formula $[Bi_2O_2][A_{m-1}B_mO_{3m+1}]$, consist of layered structured oxides in which α-PbO-type layers $[Bi_2O_2]^{2+}$ alternate with m perovskite-type layers [5]. In addition Aurivillius phases also belong to an important class of ion conductor oxides. These phases were originally studied because of their ferroelectric properties but in recent years numerous researchers have explored their oxide ion conductivity too [6].

In previous works we have evaluated the phase relations in the Bi_2O_3–TiO_2–WO_3 ternary system [7, 8]. The experimental results suggested the existence of a new phase in this system with a nominal composition close to $Bi_6Ti_5WO_{22}$. The aim of this work is to synthesize this phase as well as to obtain dense materials for its microstructural and electrical characterization.

Experimental procedure

Polycrystalline samples with nominal composition $Bi_6Ti_5WO_{22}$ were prepared by solid state reaction using high purity Bi_2O_3, TiO_2, and WO_3 (99.99%) raw materials (Alfa Aesar). Powders were mixed in a ball-mill using ethanol medium and zircona balls, then dried at 80 °C and uniaxially pressed into pellets. The pellets were calcined at 750 °C for 10 h and then reactivated by crushing and milling again. New pellets were pressed and a second treatment at 850 °C for 24 h was carried out to obtain equilibrium conditions. An additional calcining step at 1000 °C for 60 h was applied in order to obtain the pure single phase. Finally, the sintering was carried out at 1000 °C for 10 h.

The distribution of crystalline phases in the calcined specimens was determined by X-ray diffraction on powder samples (XRD, Siemens D5000, Cu kα radiation, step

T. Jardiel (✉) · A. C. Caballero · M. Villegas
Department of Electroceramics, Instituto de Cerámica y Vidrio, CSIC, Kelsen 5, Madrid 28049, Spain
e-mail: jardiel@icv.csic.es

L. Fuentes
Centro de Investigación en Materiales Avanzados, Chihuaua, Mexico

0.02). The experimental basis for the Rietveld refinement was made at the X-ray powder diffractometer located at beamline 2-1 of the Stanford Synchrotron Radiation Laboratory (SSRL), over the angular range 10–120° and with a step scan of 0.01°. The experimental data were refined using the FullProf 2k program and its graphical interface WinPLOTR [9].

In order to detect the presence of secondary phases, either non-crystalline or in small concentrations (undetectable by XRD measurements), the calcined powder as well as the sintered pellets were also analyzed with a Field Emission Scanning Electron Microscope (Hitachi S-4700) equipped with EDS (Energy Dispersive Spectroscopy).

Thermal properties in air atmosphere were determined on a Differential Scanning Calorimeter (DSC 822—Mettler-Toledo) applying a heating rate of 3 °C/min.

Electrical measurements were done on Ag electroded disks. Dielectric characterization was performed using a HP-4192A Impedance Analyzer in the following temperature ranges: −190–100 °C (using a cryostat) and 25–750 °C (using an electric furnace).

Results and discussions

Figure 1 shows the XRD diffraction pattern obtained for the B–Ti–W composition. Around 113 diffraction peaks can be observed in this spectrum and 105 of them could be assigned to the $Bi_6Ti_5WO_{22}$ phase. The remaining eight peaks are weak in intensity and correspond to $Bi_{10}Ti_3W_3O_{30}$ and also to Bi_2WO_6; actually these two Aurivillius-type phases and the $Bi_6Ti_5WO_{22}$ as well form a compatibility triangle in the Bi_2O_3–TiO_2–WO_3 phase diagram [10]. Pure single phase has not been obtained by this synthesis route. This might be related to a partial volatilization of Bi_2O_3 as it is well known to take place in other systems [11]. Furthermore, it must be noted that since this compound has been obtained very recently [7, 8] the exact stoichiometry $Bi_6Ti_5WO_{22}$ is still discussed and small deviations could easily occur.

Two different compounds exhibit an XRD pattern that completely fits the group of $Bi_6Ti_5WO_{22}$ peaks: $Bi_3(AlSb_2)O_{11}$ (JCPDF n° 86-1537) and $PbHoAl_3O_8$ (JCPDF n° 80-0046) [12, 13]. Both compounds show a cubic symmetry and a structure constituted of two interpenetrating networks, one of edge-sharing octahedra, $(AlSb_2)O_9$ or Al_3O_9 units, respectively, and one of corner-sharing octahedra, Bi_8O_4 or Pb_4LnO_7 units, respectively. These two compounds were used as a model for the structural studies of our phase.

The Rietveld refinement of the structure was carried out with the initial structural data of $Bi_3(AlSb_2)O_{11}$, $PbHoAl_3O_8$, and $Bi_6Ti_5TeO_{22}$ [12–14] phases. The lattice parameters were calculated for the peaks corresponding to the new phase, which corresponds to a cubic symmetry according to the analogous structures. According to this, the unit cell was refined with the space group Pn−3 and the refined lattice parameters were: $a = b = c = 9.4204$ (1) Å ($R_p = 17.2$, $\chi^2 = 5.41$) which are very similar to the lattice parameters reported for the $Bi_3(AlSb_2)O_{11}$, $PbHoAl_3O_8$, and $Bi_6Ti_5TeO_{22}$ cubic compounds [12–14]. The refined structural parameters are presented in Table 1, the final Rietveld plot is shown in Fig. 2 and the structure is plotted in Fig. 3.

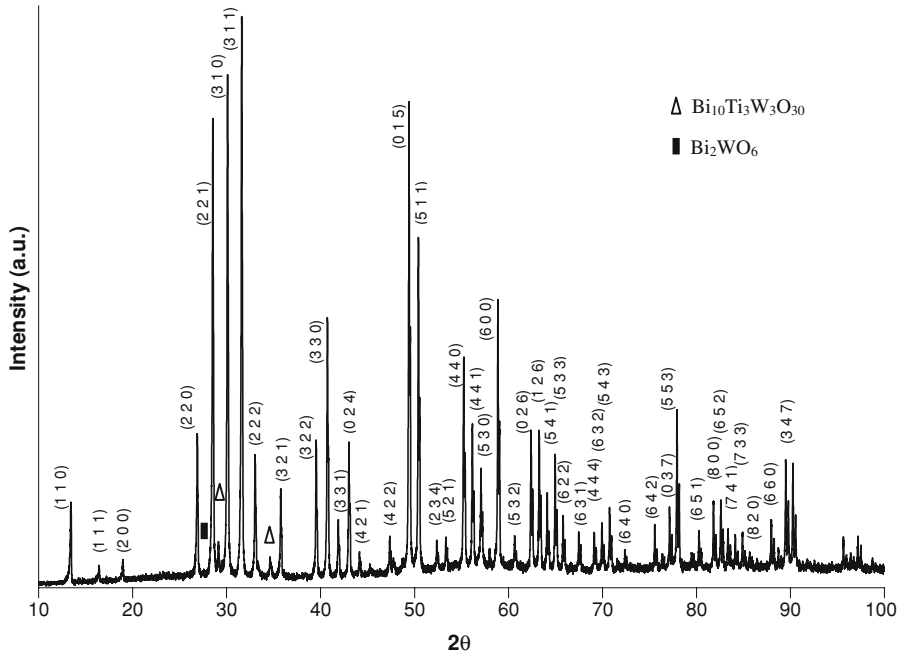

Fig. 1 XRD diffractogram for the $Bi_6Ti_5WO_{22}$ phase. All the peaks correspond to the $Bi_6Ti_5WO_{22}$ phase excepting those ascribed to Bi_2WO_6 and $Bi_{10}Ti_3W_3O_{30}$ phases

Table 1 Atomic positional and isotropic thermal parameters for $Bi_6Ti_5WO_{22}$

Atom	*x*	*y*	*z*	B
Bi(1)	0.38301(10)	0.38301(10)	0.38301(10)	1.737(32)
Bi(2)	0.00000(0)	0.00000(0)	0.00000(0)	1.737(32)
W	0.08947(44)	0.25000(0)	0.75000(0)	0.467(64)
Ti	0.08947(44)	0.25000(0)	0.75000(0)	0.467(64)
O1	0.13466(118)	0.13466(118)	0.13466(118)	0.717(224)
O2	0.25000(0)	0.25000(0)	0.87760(186)	0.717(224)
O3	0.08805(159)	0.44061(190)	0.75465(115)	0.717(224)

SEM micrograph for the sample calcined at 1000 °C/60 h is shown in Fig. 4. Two types of grains can be observed: polygonal grains and a small amount of platelet-like grains. A semi-quantitative EDS analysis (the sample morphology impeded a quantitative one) revealed a Ti/W ratio between 4:1 and 3:1 in atoms percent for the polygonal grains. This points out that these grains corresponding to the main phase present a composition close to $Bi_6Ti_5WO_{22}$. On the other hand and according to XRD results, the secondary platelets were assigned to the Aurivillius $Bi_{10}Ti_3W_3O_{30}$ and Bi_2WO_6 phases.

In order to confirm the phase evolution observed in the XRD measurements, a thermal analysis was performed on the samples calcined at 1000 °C/60 h. Figure 5 shows the DSC scan of the calcined powder, performed in air from −150 to 100 °C. As observed a change in the slope of the curve is obtained at ∼−65 °C. In the literature it is reported that $Bi_{10}Ti_3W_3O_{30}$ and Bi_2WO_6 phases do not undergo phase changes up to 705 and 665 °C, respectively, when they experiment a ferroelectric–paraelectric transition [15, 16]. The mentioned change in the slope of the DSC curve should be then associated to a phase transition of the $Bi_6Ti_5WO_{22}$ phase. One possibility is a reversible ferroelectric–paraelectric phase transition, and could be indicative of a ferroelectric nature for the synthesized phase at temperatures lower than room temperature. However when the curve is fitted to a second order polynomial, a constant value is obtained for the whole range of temperatures, which implies no changes in the material's heat capacity. Accordingly the change observed in the DCS

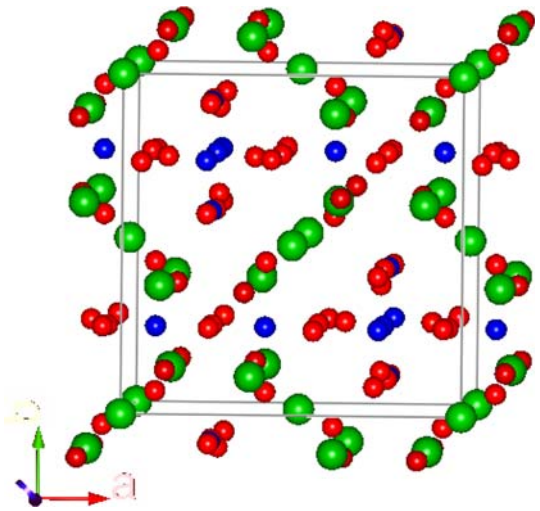

Fig. 3 Crystal structure of $Bi_6Ti_5WO_{22}$ phase

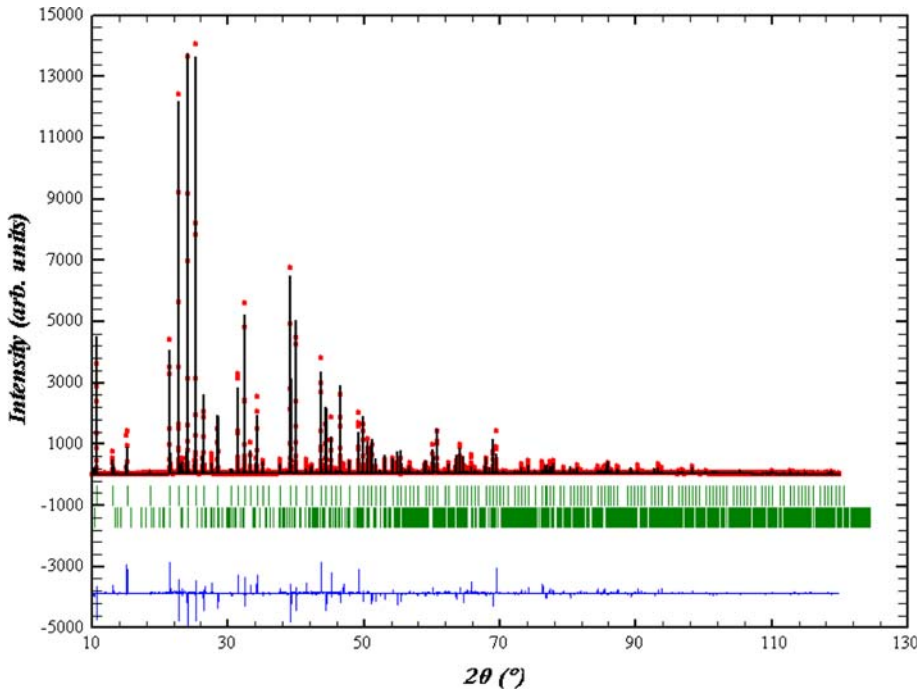

Fig. 2 Final observed, calculated, and difference plots for the XRPD Rietveld refinement

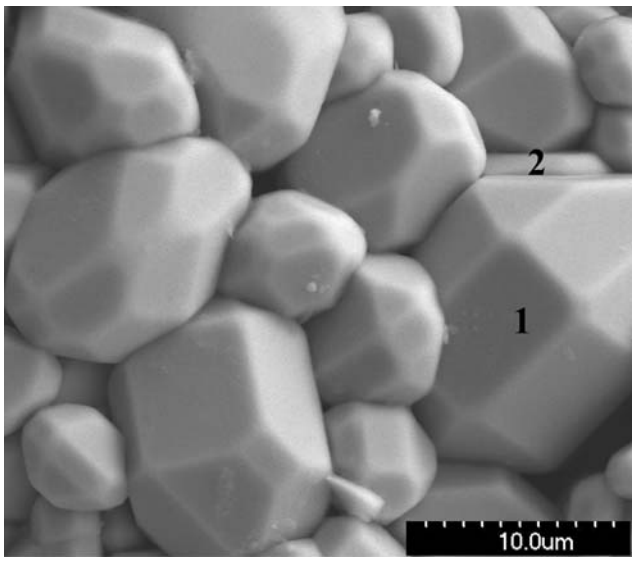

Fig. 4 SEM micrograph of the calcinated powder at 1000 °C for 60 h where it is possible to recognize two different phases: (1) $Bi_6Ti_5WO_{22}$ and (2) Aurivillius phase

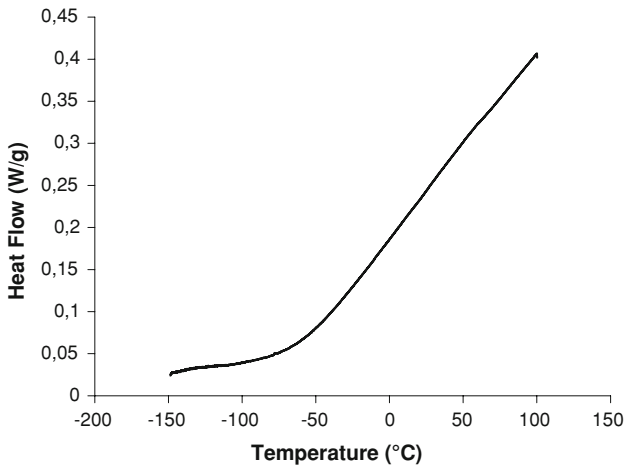

Fig. 5 DSC curve of the calcinated powder at 1000 °C for 60 h

scan should obey to a low energy order–disorder transition, rather than to a phase transition.

With regards to the electrical characterization, Fig. 6a depicts the evolution of the dielectric constant as a function of temperature at 1 MHz. One intense peak is observed around 0 °C in the dielectric constant measurements, which could only be attributed to the $Bi_6Ti_5WO_{22}$ phase. No more peaks are observed in this figure, however when representing the dielectric losses, Fig. 6b, a second peak is observed at 665 °C together with a smooth shoulder around 700 °C. As mentioned these temperatures correspond to the ferroelectric–paraelectric phase transitions of the Bi_2WO_6 and the $Bi_{10}Ti_3W_3O_{30}$ Aurivillius phases, respectively.

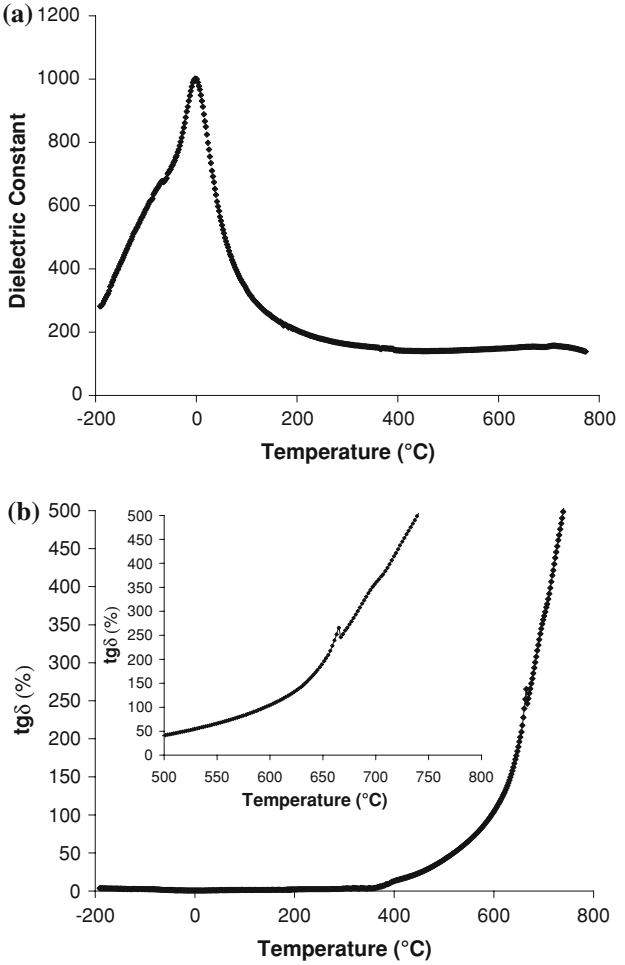

Fig. 6 Dielectric constant and dielectric losses as a function of temperature at 1 MHz for the sintered material

Finally Fig. 7 represents the evolution of the dielectric constant with temperature at different frequencies. As observed the peak at 0 °C is in fact constituted by two peaks, one centered at 3 °C and the other one changing its position with the frequency, from −44 °C at 1 kHz to −37 °C at 1 MHz. However, this is not a relaxor-like behavior and is very similar to that observed in barium titanate-based dielectric materials. In these materials, a diffuse phase transitions take place due to chemical inhomogeneities or stress induced by core–shell structures within the barium titanate grains [17, 18]. In the proposed complex structure of the $Bi_6Ti_5WO_{22}$ phase, with two interpenetrating networks, it could be possible that a certain degree of local heterogeneities and compositional gradients might form in the grains. If this is so, as it is the case for high permittivity barium titanate-based dielectric materials, a diffuse phase transition could be expected originated by either core–shell structures or the presence of compositionally different clusters.

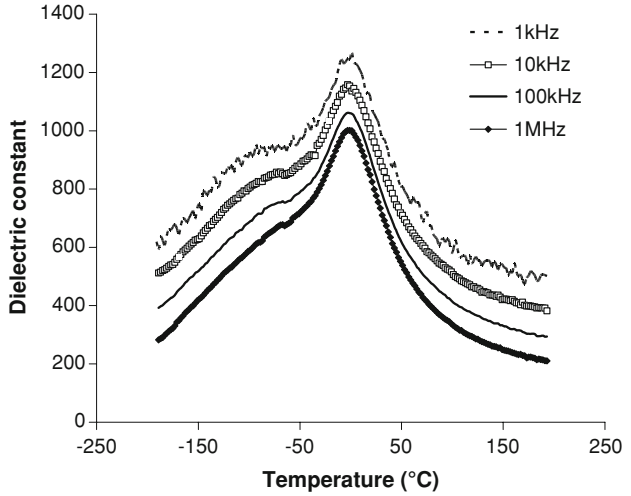

Fig. 7 Dielectric constant as a function of temperature at different frequencies for the sintered material

Conclusions

A new bismuth titanate phase with stoichiometry close to $Bi_6Ti_5WO_{22}$ has been observed in the Bi_2O_3–TiO_2–WO_3 ternary system. This new phase has a structure similar to $Bi_3(AlSb_2)O_{11}$ and $PbHoAl_3O_8$ phases, which show a cubic symmetry at room temperature. The compound could not be obtained as a single phase and traces of $Bi_{10}Ti_3W_3O_{30}$ and Bi_2WO_6 Aurivillius-type phases were also present in the synthesized material. DSC analyses however showed no phase transitions in the temperature range between −150 and 100 °C. The electrical characterization shows two peaks in the dielectric response. One, positioned around 665 °C, is in fact formed by a peak and a shoulder which are attributed to the Bi_2WO_6 and $Bi_{10}Ti_3W_3O_{30}$ Aurivillius traces. The main peak, centered at 0 °C, is attributed to the $Bi_6Ti_5WO_{22}$ phase and is also constituted by a couple of peaks. The dielectric response with the frequency of these two peaks points out to an order–disorder transition in the $Bi_6Ti_5WO_{22}$ phase similar to that of $BaTiO_3$-based materials.

Acknowledgements Portions of this research were carried out at the Stanford Synchrotron Radiation Laboratory, a national user facility operated by Stanford University on behalf of the U.S. Department of Energy, Office of Basic Energy Sciences.

References

1. Subbarao EC (1965) J Phys Chem Solids 23:665
2. Scott JF, Araujo CA (1989) Science 246:1400
3. Jardiel T, Caballero AC, Villegas M (2008) J Ceram Soc Jpn 116:511
4. Shrout TR, Eitel R, Randall C (2002) In: Setter N (ed) Piezoelectric materials in devices. EPFL Swiss Federal Institute of Technology, Lausanne, Switzerland, 413 pp
5. Aurivillius B (1950) Ark Kemi 1:499
6. Kendall KR, Navas C, Thomas JK, Zur Loye HC (1996) Chem Mater 8:642
7. Jardiel T, Caballero AC, Villegas M, Valant M, Jancar B, Suvorov D (2006) J Eur Ceram Soc 26:2931
8. Jardiel T, de la Rubia MA, Peiteado M (2008) J Am Ceram Soc 91:1083
9. Rodríguez-Carvajal JT (2005) FullProf.2K (Version 3.40). Rietveld, profile matching and integrated intensity refinement of X-ray and/or neutron data (Multi_Pattern: WindowsConsole-version, Nov 2005)
10. Jardiel T, Villegas M, Caballero A, Suvorov D, Caballero AC (2008) J Am Ceram Soc 91:278
11. Peiteado M, de la Rubia MA, Velasco MJ, Valle JF, Caballero AC (2005) J Eur Ceram Soc 25:1675
12. Ismunandar, Kennedy BJ, Hunter BA (1996) J Solid State Chem 127:178
13. Scheikowski M, Müller-Buschbaum HK (1993) Z Anorg Allg Chem 619:1755
14. Udovic M, Valant M, Jancar B, Suvorov D, Meden A, Kocevar A (2006) J Am Ceram Soc 89:3462
15. Kharitonova EP, Voronkova VI (2007) Inorg Mater 43:1340
16. Knight KS (1993) Ferroelectrics 150:319
17. Park Y, Kim Y (1995) J Mater Res 10:2770
18. Rawal BS, Kahn M, Buessem WR (1981) In: Advances in ceramics, vol 1. The American Ceramic Society, Columbus, Ohio, 172 pp